1180 *Inorg. Chem.* **1989**, *28*, 1180-1183

Contribution from the Department of Chemistry and
Laboratory for Molecular Structure and Bonding, Texas A&M University, College Station, Texas 77843

Electronic Structures of the $Ru_2(RNNNR)_4$, $Rh_2(RNCHNR)_4$, and $Co_2(RNNNR)_4$ Molecules: Ordering and Separation of M–M δ^* and π^* Orbitals

F. Albert Cotton* and Xuejun Feng

Received November 11, 1988

The electronic structures of $Ru_2(RNNNR)_4$, $Rh_2(RNCHNR)_4$, and $Co_2(RNNNR)_4$ (R = p-$CH_3C_6H_4$) have been investigated by means of Xα–SW molecular orbital calculations on model molecules in which the R group is replaced by a hydrogen atom. It is found that in these molecules the energy of the M–M antibonding δ^* orbital is considerably higher than that of the antibonding π^* orbital. Thus, the calculated electronic configuration for $Ru_2(RNNNR)_4$, $\sigma^2\pi^4\delta^2\pi^{*4}$, provides an excellent explanation for the structural features and the diamagnetism of the molecule. The large π^*–δ^* gap in these molecules has been shown to be the consequence of the strong interaction between the δ^* orbital of the M_2^{4+} unit and the pπ lone pair of the ligands. Such a strong interaction in these molecules, compared to the case in their carboxylate analogues, is determined by the electronic properties of the $RNCHNR^-$ and $RNNNR^-$ ligands.

Introduction

Transition-metal complexes that contain an M_2 unit embraced by four bent, triatomic, uninegative, bridging bidentate ligands, to give an $M_2(LL)_4$ or $M_2(LL)_4X_{1,2}$ molecule, are numerous and important.[1] The most common such ligands are carboxylate ions, $OCRO^-$, amido ions, $RNCR'O^-$, amidinato ions, $RNCR'NR''^-$, and triazenato ions, $RNNNR^-$. In general, the electronic properties of the $RNCR'NR''^-$ and $RNNNR^-$ ions are similar, but these ligands differ from the carboxylate and amidinato ions.[2,3] It is well-known that, because of the differences, the latter ligands have quite different effects on certain properties of the M_2^{n+} unit they encapsulate. Indeed, the $RNCR'NR''^-$ and $RNNNR^-$ ligands can stabilize M_2^{n+} units that do not occur with the carboxylate or amido ligands, e.g., the diamagnetic Co–Co-bonded Co_2^{4+} unit.[2]

In a recent paper[4] we reported a new compound, $Ru_2(RNNNR)_4$, where R = p-$CH_3C_6H_4$. The most important feature of this molecule, compared to its carboxylate analogues,[1] is its diamagnetism. This feature, together with certain of its structural features, led to the conclusion that the electron configuration representing the M–M interaction in this molecule is $\sigma^2\pi^4\delta^2\pi^{*4}$. This requires that, in contrast to the known electronic structure of the diruthenium carboxylate compounds,[5] the δ^* orbital not only be higher than the π^* orbital but also be well separated from it.

This conclusion, based solely on the experimental data, will be further considered, and confirmed, in this paper by an SCF–Xα–SW calculation on the compound. The electronic structures of two other compounds, $Rh_2(RNCHNR)_4$[6] and $Co_2(RNNNR)_4$[2] (R = p-$CH_3C_6H_4$), will also be studied by means of Xα–SW calculations. With the results of these calculations we will present a systematic discussion of the relative ordering and separation of the M–M antibonding δ^* and π^* orbitals in molecules of this type.

Computational Methods

The electronic structures of $Ru_2(RNNNR)_4$, $Rh_2(RNCHNR)_4$, and $Co_2(RNNNR)_4$ were calculated by employing model systems in which the R groups (R = p-$CH_3C_6H_4$) were replaced by hydrogen atoms. The legitimacy of this simplification has been demonstrated elsewhere.[7] The calculations were performed by the SCF–Xα–SW method.[8a] Overlapping atomic sphere radii were taken to be 88.5% of the atomic number radii[8b] for the Ru and Co compounds and 89% for the Rh compound. In all calculations, the starting molecular potential was a superposition of neutral atomic Herman–Skillman potentials[8c] and α values were taken from the compilation of Schwarz.[8d]

The atomic coordinates used in the calculations were determined from the crystallographic bond distances and angles of the real molecules, except for C–H and N–H distances, which were taken as 1.08 and 1.06 Å, respectively. D_{4h} symmetry was assumed in the calculations of the three molecules. For $Rh_2(HNCHNH)_4$ and $Co_2(HNNNH)_4$, their staggered conformations with a torsional angle of ca. 17° were also taken into account by performing the calculations in D_4 symmetry.

Results and Discussion

$Ru_2(HNNNH)_4$. The properties of the $Ru_2(RNNNR)_4$ molecule have been reported and discussed in a previous paper.[4] The structure of the molecule has two notable features. It is strictly eclipsed, and the Ru–Ru bond distance is 2.417 (2) Å. This is much longer than that in $Ru_2(O_2CR)_4$ molecules, viz., about 2.27 Å.[9] The ^1H NMR spectrum shows clearly that the molecule is diamagnetic. The facts have led to the assignment of a $\sigma^2\pi^4\delta^2\pi^{*4}$ configuration to the molecule. As will be seen below, the prediction of the electronic structure is well confirmed by the present Xα–SW calculation.

The calculated results for $Ru_2(HNNNH)_4$ are shown in Table I. Listed there are the energies and relative amounts of charge within the atomic spheres for the upper valence molecular orbitals. There are also 20 lower lying valance MO's that are almost completely ligand-based. The orbitals are not of interest in the present discussion and, therefore, are not shown. The MOs listed in Table I may be divided into three groups. The group of orbitals that have only negligible or no metal character are essentially the N lone pairs or the π orbitals of the ligands. The metal–ligand bonds are represented by the group of MOs that pick up appreciable amounts of metal character (up to 42%). The third group of orbitals are those that have more than 60% metal contribution, and they may be best classified as the M–M bonding and antibonding MOs. The MOs in the last group are, in order of increasing energy, $4a_{1g}$ (σ), $5e_u$ (π), $2b_{2g}$ (δ), $5e_g$ (π^*), $2b_{1u}$ (δ^*), and $4a_{2u}$ (σ^*). It may be mentioned that the $5a_{1g}$ orbital also has M–M σ-bonding character but it is at the same time Ru–N antibonding.

A remarkable feature of the electronic structure of $Ru_2(HNNNH)_4$ as shown in Table I is that the HOMO is a fully occupied π^* orbital and it is far below the LUMO (δ^*) by ca. 1 eV. Thus,

---

(1) Cotton, F. A.; Walton, R. A. *Multiple Bonds between Metal Atoms*; Wiley: New York, 1982.

(2) Cotton, F. A.; Poli, R. *Inorg. Chem.* **1987**, *26*, 3652.

(3) Cotton, F. A.; Feng, X. Unpublished work on the electronic structures of O_2CH^-, $HNCHNH^-$, and $HNNNH^-$ by an ab initio Hartree–Fock method.

(4) Cotton, F. A.; Matusz, M. *J. Am. Chem. Soc.* **1988**, *110*, 5761.

(5) Norman, J. G., Jr.; Renzoni, G. E.; Case, D. A. *J. Am. Chem. Soc.* **1979**, *101*, 5256.

(6) Piraino, P. P.; Bruno, G.; Schiavo, S. L.; Laschi, F.; Zanello, P. *Inorg. Chem.* **1987**, *26*, 2205.

(7) Cotton, F. A.; Feng, X.; Matusz, M. *Inorg. Chem.* **1989**, *28*, 594.

(8) (a) Slater, J. C. *Quantum Theory of Molecules and Solid*; McGraw-Hill: New York, 1974; Vol. IV. (b) Norman, J. G.; Jr. *Mol. Phys.* **1976**, *31*, 1191. (c) Herman, F.; Skillman, S. *Atomic Structure Calculations*; Prentice-Hall: Englewood Cliffs, NJ, 1963. (d) Schwarz, K. *Phys. Rev. B* **1972**, *5*, 2466.

(9) Lindsay, A. J.; Wilkinson, G.; Motevalli, M.; Hursthouse, M. B. *J. Chem. Soc., Dalton Trans.* **1985**, 2321.

Table I. Upper Valence Molecular Orbitals for $Ru_2(HNNNH)_4$

		% contribn			Ru angular contribn		
D_{4h} level	energy, eV	2 Ru	12 N	8 H			
$4a_{2u}$	−4.447	91	7	2	5% s	5% p	90% d_{z^2}
$2b_{1u}$	−4.938	69	31	0			100% d_{xy}
$5e_g$[a]	−5.894	96	3	1			100% $d_{xz,yz}$
$1a_{1u}$	−6.632	0	100	0			
$6e_u$	−6.952	24	69	7		21% p	79% $d_{xz,yz}$
$2b_{2g}$	−7.034	80	20	0			100% d_{xy}
$4e_g$	−7.244	1	99	0			
$5a_{1g}$	−7.657	52	46	2	37% s	2% p	61% d_{z^2}
$5e_u$	−7.768	79	21	0		1% p	99% $d_{xz,yz}$
$4b_{1g}$	−9.062	29	68	3			100% $d_{x^2-y^2}$
$4a_{1g}$	−9.159	61	37	2		1% p	99% d_{z^2}
$1b_{1u}$	−9.340	42	58	0			100% d_{xy}
$3e_g$	−9.924	8	79	13			
$1a_{2g}$	−11.017	0	100	0			
$4e_u$	−11.420	0	100	0			
$3a_{2u}$	−11.606	20	62	18	34% s	1% p	65% d_{z^2}
$3b_{2u}$	−11.884	27	55	18			100% $d_{x^2-y^2}$
$1b_{2g}$	−12.256	10	90	0			100% d_{xy}

[a] The highest occupied molecular orbital.

Table II. Upper Valence Molecular Orbitals for $Rh_2(HNCHNH)_4$ and $Co_2(HNNNH)_4$

$Rh_2(HNCHNH)_4$									$Co_2(HNNNH)_4$							
D_{4h} level	energy, eV	% contribn				Rh angular contribn			D_{4h} level	energy, eV	% contribn			Co angular contribn		
		2 Rh	8 N	4 C	12 H						2 Co	12 N	8 H			
$4a_{2u}$	−5.509	89	9	0	2	5% s	4% p	91% d_{z^2}	$2b_{1u}$	−5.588	74	26	0			100% d_{xy}
$2b_{1u}$[a]	−5.552	51	49	0	0			100% d_{xy}	$4a_{2u}$[a]	−5.611	95	4	1	3% s	3% p	94% d_{z^2}
$1a_{1u}$	−6.019	0	100	0	0				$1a_{1u}$	−6.228	0	100	0			
$5e_g$	−6.595	2	98	0	0				$5e_g$	−6.395	97	2	1			100% $d_{xz,yz}$
$4e_g$	−7.220	96	2	1	1			100% $d_{xz,yz}$	$4e_g$	−6.956	3	97	0			
$2b_{2g}$	−7.363	81	8	11	0			100% d_{xy}	$2b_{2g}$	−6.998	90	10	0			100% d_{xy}
$6e_u$	−7.976	22	53	7	18		27% p	73% $d_{xz,yz}$	$6e_u$	−7.221	74	22	4		3% p	97% $d_{xz,yz}$
$5a_{1g}$	−8.700	68	19	5	8	30% s	2% p	68% d_{z^2}	$5e_u$	−7.647	36	61	3		14% p	86% $d_{xz,yz}$
$5e_u$	−8.748	81	11	5	3		1% p	99% $d_{xz,yz}$	$5a_{1g}$	−8.061	93	7	0	13% s	2% p	85% d_{z^2}
$1b_{1u}$	−9.381	65	35	0	0			100% d_{xy}	$4b_{1g}$	−8.803	37	59	4			100% $d_{x^2-y^2}$
$1a_{2g}$	−9.458	0	67	33	0				$4a_{1g}$	−8.810	24	71	5	20% s		80% d_{z^2}
$3e_g$	−9.758	8	78	2	12				$1b_{1u}$	−8.939	42	58	0			100% d_{xy}
$4e_u$	−10.130	3	65	29	3				$3e_g$	−10.378	9	74	17			
$4a_{1g}$	−10.578	49	22	11	18	2% s		98% d_{z^2}	$1a_{2g}$	−11.182	0	100	0			
$4b_{1g}$	−10.806	38	25	14	23			100% $d_{x^2-y^2}$	$3b_{2u}$	−11.311	29	54	17			100% $d_{x^2-y^2}$
$1b_{2g}$	−11.269	26	55	19	0			100% d_{xy}	$4e_u$	−11.646	0	100	0			
$3a_{2u}$	−11.754	25	58	0	17	30%	1% p	69% d_{z^2}	$3a_{2u}$	−11.763	17	60	23	46% s		54% d_{z^2}
$3b_{2u}$	−12.126	34	49	0	17			100% $d_{x^2-y^2}$	$1b_{2g}$	−12.426	6	94	0			

[a] The highest occupied molecular orbital.

the M–M bonding orbitals have the familiar order predicted on a qualitative basis.[1] The order of the δ^* and π^* orbitals, their antibonding counterparts, however, is reversed as compared to that familiar order. The electron configuration describing the M–M interaction is thus clearly predicted by the calculation as $\sigma^2\pi^4\delta^2\pi^{*4}$, leading to a double bond between the pair of metal atoms.

The results of the present calculation provide an excellent explanation for the structural features and the diamagnetic nature of the $Ru_2(RNNNR)_4$ molecule. The presence of the net δ bond is in full accord with the eclipsed configuration of the molecule. The Ru–Ru distance being much longer than those in the carboxylate species,[9] which are about 2.27 Å, is obviously due to complete loss of the π bonds. The large π^*–δ^* energy gap indicates that the δ^* orbital is inaccessible thermally at room temperature and leads to a singlet ground state for the molecule.

It is interesting to compare the present results to the electronic structure calculated for the $Ru_2(O_2CR)_4$ compounds.[5] The MO diagrams of the carboxylate compounds[5] show a pattern generally similar to that in Table I, but several significant differences can be easily observed. One of the most notable differences is that in the carboxylate compounds the energy of the δ^* orbital is only slightly higher than that of the π^* orbital. This feature has provided a qualitative theoretical basis for the paramagnetic nature of both $Ru_2(O_2CR)_4$ and $Ru_2(O_2CR)_4X$ compounds. The reversed order of the δ^* and π^* orbitals was explained by Norman et al.[5] as due to the Ru–O antibonding character in the δ^* orbital arising from interaction between the metal δ^* d-orbital combination and the pπ lone pairs on oxygen. Such an interaction should be much stronger in the case of $Ru_2(HNNNH)_4$ as indicated by the larger π^*–δ^* energy gap. We will return to this point later in detail.

$Rh_2(HNCHNH)_4$ and $Co_2(HNNNH)_4$. Let us consider the calculation for the Rh compound first. It is interesting to note that the $Rh_2(HNCHNH)_4$ molecule has two more electrons than $Ru_2(HNNNH)_4$, and the ligands of the two molecules have very similar electronic properties. Thus, the electronic structure of $Rh_2(HNCHNH)_4$ might be deduced from that of $Ru_2(HNNNH)_4$ by adding two electrons to the empty δ^* orbital of the Ru compound. This is essentially the case. As shown in the left side of Table II, the MO diagram of $Rh_2(HNCHNH)_4$ calculated in D_{4h} symmetry has a structure similar to that of $Ru_2(HNNNH)_4$, and a single σ bond between the Rh atoms is predicted. However, there are a few points about the MO diagram that deserve further comment.

It is evident that in $Rh_2(HNCHNH)_4$ the $2b_{1u}$ orbital, which is the HOMO and is correlated to the δ^* orbital of $Ru_2(HNNNH)_4$, has only 50% metal character, while the $1b_{1u}$ orbital has 65%. The two orbitals are a bonding–antibonding pair arising from strong interaction between the δ^* orbital of Rh_2^{4+} and the nitrogen pπ lone pair of the ligands. As we will see below, the interaction seems to be overestimated by the Xα–SW calculations for systems of this type. Consequently, if we still regard the $2b_{1u}$

orbital as the main δ^* orbital for the convenience of discussion, the energy gap between the σ^* ($4a_{2u}$ and LUMO) and δ^* orbitals is only 0.04 eV compared to 0.49 eV in $Ru_2(HNNNH)_4$ whereas the $\pi^*(4e_g)$–δ^* gap is increased from 0.95 eV in $Ru_2(HNNNH)_4$ to 1.67 eV. It is also to be noted that both $4a_{1g}$ and $5a_{1g}$ orbitals have M–M σ-bonding character. But now it is the $5a_{1g}$ orbital that is mainly responsible for the σ bond. The Rh–N antibonding character of the $5a_{1g}$ orbital causes it to be even higher than the π ($5e_u$) orbital. The calculation of $Rh_2(HNCHNH)_4$ in D_4 symmetry affords a result quite similar to that just discussed, except for a smaller π^*–δ^* gap (1.51 eV) and a larger δ^*–σ^* gap (0.16 eV). Beyond this, no further discussion seems necessary.

The $Rh_2(HNCHNH)_4$ molecule has been previously calculated by the DV–Xα method.[10] The calculation, supported by photoelectron spectroscopy, indicated that the HOMO of the molecule should be an orbital with predominant δ^* character. The π^*–δ^* and δ^*–σ^* energy gaps obtained in this calculation are 1.04 and 0.46 eV, respectively. It is noted that the ionization potential of an electron in the δ^* orbital predicted by this calculation is 0.84 eV less than the experimental value, which implies that the calculated δ^* level there is higher than it should be. If we keep this in mind and consider also the energy gaps in $Ru_2(HNNNH)_4$, the $2b_{1u}$ level in our Xα–SW calculation for $Rh_2(HNCHNH)_4$ might be about 0.3 eV too high due to the overestimated interaction. It may be mentioned that even when this is taken into account the π^*–δ^* separation is still considerably greater than the separation in its carboxylate analogue, $Rh_2(O_2CH)_4$.[11]

Let us now turn to the $Co_2(HNNNH)_4$ molecule, which, like $Rh_2(HNCHNH)_4$, also contains a d^7–d^7 M_2 unit with a single bond. The Co–Co distance, 2.265 Å, is much shorter than the Ni–Ni distance, 2.485 Å, in $Ni_2(RNCHNR)_4$, where it has been shown that no M–M bond exists.[12] Thus, the MO scheme describing the M–M interaction in $Co_2(HNNNH)_4$ was expected[2] to be $\sigma^2\pi^4\delta^2\pi^{*4}\delta^{*2}$, which would provide a net single σ bond between the metal atoms.

However, the result of the present Xα–SW calculation is not directly in accord with this expectation. As seen in the right part of Table II, the calculation gives for the HOMO ($4a_{2u}$) of $Co_2(HNNNH)_4$ a σ^* orbital, whereas the LUMO ($2b_{1u}$) is a δ^* orbital. In addition, the HOMO and the LUMO are nearly degenerate, separated by only 0.02 eV. The result is obviously inconsistent with the structural features of the molecule. The molecule was also calculated in D_4 symmetry, which took into account twisting of the molecule away from the eclipsed conformation. However, this calculation could even not be converged because of the close spacing of the HOMO and LUMO levels unless both levels were required to be singly occupied. This is obviously not the case, since experimentally the molecule is not paramagnetic.

The unexpected ordering and separation of the δ^* and σ^* orbitals may again be understood through the overestimated Co–N interaction discussed in the $Rh_2(HNCHNH)_4$ case. The interaction may cause the $2b_{1u}$ orbital, which is also Co–N antibonding in character, to be pushed too high. A similar case of reversed order of the δ^* and σ^* orbitals can also be seen for $Ni_2(HNCHNH)_4$.[12] It is noted that except for the HOMO and the LUMO the nature of all other MOs of $Co_2(HNNNH)_4$ in Table II is just as expected. Therefore, if the overestimated interaction could be removed, the δ^* orbital might then be brought down by a few tenths of an electronvolt and we would surely have a $\sigma^2\pi^4\delta^2\pi^{*4}\delta^{*2}$ configuration with a reasonably large σ^*–δ^* gap. Such a configuration would be consistent not only with the Co–Co distance (owing to the existence of a σ bond) but also with the staggered conformation because of the lack of the δ bond.

π^*–δ^* Separation. The electronic structures of the compounds we have just discussed have a common feature, namely, that the M–M antibonding δ^* orbital is considerably higher in energy than the antibonding π^* orbital. Such a feature has been shown to be crucial in understanding the diamagnetic nature and long Ru–Ru distance in $Ru_2(HNNNH)_4$. It has been pointed out that the destabilization of the δ^* orbital is due to the M–N antibonding character in the orbital that arises from the interaction of the metal d-orbital combination of δ^* type with the pπ lone pair of the ligands. As we have seen, for a given metal dimer the strength of the interaction is affected by the nature of the ligands. Let us consider this from the point of view of the different electronic properties of the ligands first.

Table III. Energy Difference between the $2b_{1u}$ and π^* Orbitals and Metal Character in the $2b_{1u}$ and $1b_{1u}$ Orbitals

		% metal character	
molecule	ΔE, eV[a]	$2b_{1u}$	$1b_{1u}$
$Mo_2(O_2CH)_4$[b]	−1.34	86	14
$Mo_2(HNCHNH)_4$[c]	−1.04	77	31
$Ru_2(O_2CH)_4^+$[d]	0.26	69	37
$Rh_2(O_2CH)_4$[e]	0.37	68	39
$Ru_2(HNNNH)_4$	0.95	69	42
$Rh_2(HNCHNH)_4$	1.67	51	65
$Pd_2(HNCHNH)_4$[f]	2.31	38	77

[a] $\Delta E = E(2b_{1u}) - E(\pi^*)$. [b] Norman, J. G., Jr.; Kolari, H. J.; Gray, H. B.; Trogler, W. C. *Inorg. Chem.* **1977**, *16*, 987. [c] See ref 7. [d] See ref 5; for $Ru_2(O_2CH)_4$ ΔE is even smaller. [e] See ref 11. [f] See ref 12.

It is well-known that the ligands have an increasing ability, in the order $RNCHNR^- \simeq RNNNR^- > OCR'O^-$, to strengthen the M–M interaction for a given M_2^{4+} unit.[2] This property may depend upon the donor strength of the ligands, especially the σ donor strength, which determines the metal–ligand bonds in the compounds. Such a property of the ligands is one of the factors determining the Cr–Cr bond strength in dichromium complexes.[13] Another difference between these ligands that is of interest in the present case may be seen through the electronic structure of the ligands. Calculations[3] show that the HOMOs of all these ligands, namely, $HNCHNH^-$, $HNNNH^-$, and $OCHO^-$, are the same in character but very different in energy. The HOMO is a pπ lone-pair orbital of a_2 symmetry with electron density localized on the N or O atoms at the ends. The energy of the orbital is much lower in $OCHO^-$ than in $HNCHNH^-$ and $HNNNH^-$, but the energies are quite similar in the last two cases. Four such pπ lone-pair orbitals should be expected in D_{4h} symmetry of the molecular frames, namely, a b_{1u} orbital, an a_{1u} orbital, and a doubly degenerate e_g orbital. Thus, the pπ lone-pair orbital of the b_{1u} type would be expected to interact with the δ^* d-orbital combination of the metal dimer of the same symmetry. The interaction results in the $1b_{1u}$ and $2b_{1u}$ orbitals as seen in Tables I and II, which have metal–ligand bonding and antibonding character, respectively. Obviously, better energy matching between the metal orbital and the nitrogen pπ lone pair in $HNCHNH^-$ and $HNNNH^-$ would lead to a stronger interaction.

In Table III we list the energy difference between the $2b_{1u}$ and π^* orbitals as well as the metal character in the $2b_{1u}$ and $1b_{1u}$ orbitals for some molecules that were calculated in previous studies or in this work. The table shows an interesting relationship of the increasing energy difference against the decreasing metal character in the $2b_{1u}$ orbital and increasing metal character in the $1b_{1u}$ orbital. It can be seen that, for any pair of molecules of the same metal dimer but different ligands, the energy difference always has a considerably larger value in the molecule with non-carboxylate ligands. This fact as well as the greater metal character of the $1b_{1u}$ orbital indicates clearly a stronger metal–ligand interaction in the molecules with amidinato or triazenato ligands. It is also interesting to compare a pair of molecules where they have the same or similar ligands but a different dimetal unit. In such a case the energy difference is always larger in the molecule that has the metal atoms of higher atomic number. This

---

(10) Rizzi, G. A.; Casarin, M.; Tondello, E.; Piraino, P.; Granozzi, G. *Inorg. Chem.* **1987**, *26*, 3406.

(11) Norman, J. G., Jr.; Kolari, H. J. *J. Am. Chem. Soc.* **1978**, *100*, 791.

(12) Cotton, F. A.; Matusz, M.; Poli, R.; Feng, X. *J. Am. Chem. Soc.* **1988**, *110*, 1144.

(13) Cotton, F. A.; Ilsley, W. H.; Kaim, W. *J. Am. Chem. Soc.* **1980**, *102*, 3464.

may be easily understood through the drop in energy of the metal d orbitals from Mo_2^{4+} to Rh_2^{4+}, which leads again to a better energy matching between the δ^* orbital of the metal dimer and the ligand pπ lone pair. In the $Pd_2(HNCHNH)_4$ molecule[12] the d orbitals in Pd_2^{4+} may have become even lower than the ligand orbital so that the interaction causes the lower lying $1b_{1u}$ orbital to be mostly δ^* in character.

Finally it may be noticed that the π^* orbital (e_g type in D_{4h} symmetry) of the metal dimers might also be matched well in energy with the ligand pπ lone pair of e_g symmetry, so that interaction between them could be expected in some molecules. However, the calculations for all compounds concerned in this work show that such an interaction is nearly or completely negligible. The reason for this is simple. The relative orientation of the π^* orbital and the e_g pπ lone pair is unfavorable for any significant overlapping between them. Therefore, no interesting interaction should be expected.

Acknowledgment. We thank the National Science Foundation for support.

Contribution from the Institute of Chemistry, University of Wrocław, 50 383 Wrocław, Poland, and Department of Chemistry, University of California, Davis, California 95616

Five-Coordinate Complexes of 21-Thiaporphyrin. Preparations, Spectra, and Structures of Iron(II), Nickel(II), and Copper(II) Complexes

Lechosław Latos-Grażyński,[*,†] Jerzy Lisowski,[†] Marilyn M. Olmstead,[‡] and Alan L. Balch[*,‡]

Received October 14, 1988

Insertion of Fe(II), Ni(II), and Cu(II) as their chloride salts into tetraphenyl-21-thiaporphyrin, STPPH, yields $Fe^{II}(STPP)Cl$ ($S = 2$, $\mu_{eff} = 5.2\ \mu_B$), $Ni^{II}(STPP)Cl$ ($S = 1$, $\mu_{eff} = 3.3\ \mu_B$), and $Cu^{II}(STPP)Cl$ ($S = {}^1/_2$). Electronic spectra of these complexes show porphyrin-like behavior with a strong Soret peak at 400 nm. The Mössbauer spectrum for $Fe^{II}(STPP)Cl$ (QS = 3.93 mm/s, IS = 0.88 mm/s at 295 K) is characterized by a large quadrupolar splitting found for related high-spin iron(II) complexes. The structures of these three isomorphous compounds (triclinic, $P\bar{1}$) have been determined by X-ray diffraction: $Fe^{II}(STPP)Cl(CH_3CN)$, $a = 10.059$ Å, $b = 13.661$ (4) Å, $c = 15.033$ (5) Å, $\alpha = 102.53$ (2)°, $\beta = 104.16$ (2)°, $\gamma = 106.37$ (2)°, $Z = 2$ at 130 K, least-squares refinement of 240 parameters using 3034 reflections, $R = 0.077$; $Ni^{II}(STPP)Cl$, $a = 10.154$ (3) Å, $b = 13.687$ (4) Å, $c = 15.064$ (4) Å, $\alpha = 101.97$ (2)°, $\beta = 103.62$ (2)°, $\gamma = 105.90$ (2)°, $Z = 2$ at 293 K, least-squares refinement of 489 parameters with 4860 reflections, $R = 0.053$; $Cu^{II}(STPP)Cl(CH_3CN)$, $a = 10.061$ (6) Å, $b = 13.646$ (7) Å, $c = 14.930$ (8) Å, $\alpha = 102.12$ (4)°, $\beta = 104.02$ (4)°, $\gamma = 108.20$ (4)°, $Z = 2$ at 130 K, least-squares refinement of 228 parameters with 3951 reflections, $R = 0.084$. The complexes share a basic five-coordinate structure with approximately square-pyramidal geometry and an apical chloride. The thiophene ring is bent from the plane of the remainder of the $STPP^-$ ligand core and is η^1-bound to the metal through a pyramidal sulfur.

Introduction

The porphyrin core is well recognized as providing a stable yet somewhat flexible environment for the coordination of a great variety of metal ions. In recent years the modification of that core has attracted attention for a variety of reasons.

Addition of substituents to one of the nitrogens to give an *N*-alkylporphyrin (**1**) has become significant in a biological context, and this represents a significant pathway for physiological porphyrin destruction.[1] Insertion of an oxygen atom into a porphyrin N–metal bond to give a complex of a porphyrin *N*-oxide (**2**) may be a significant reaction in oxygen atom transfer and oxidation processes.[2] Insertions of carbenes or nitrenes into N–M bonds, which have been observed in model systems, may be related by other biological examples of porphyrin destruction.[3]

Modification of porphyrins by introduction of other atoms (O, S, Se) for one or more of the pyrrole nitrogens produces new macrocycles that are of interest for use as new complexing agents and for theoretical reasons. In the latter regard, the tetraoxaporphyrin dication **3** has recently been synthesized and discussed in the context of the aromatic character of annulenes.[4] Limited reports on the oxaporphyrin **4**,[5] dithiaporphyrin **5**,[6] and diselenaporphyrin **6**[6] have appeared. We recently reported a reasonable synthesis of tetra-*p*-tolyl-21-thiaporphyrin (**7**, STTPH) and determined its structure and that of its copper(II) bicarbonate complex.[7] The thiaporphyrin incorporates one thiophene ring in its core. Thiophene–transition-metal bonding can occur in several fashions: S bound, C bound, or η^5 bound.[8] Moreover, the thiophene–transition-metal bond appears to be relatively weak but very important to the process of hydrodesulfurization.[9] Therefore, it is of interest to examine the effect of the thiophene ring on the coordination of metal ions by **7**. Here we report on the structures and spectroscopic properties of complexes of **7** with iron(II), nickel(II), and copper(II) and comment on the structural

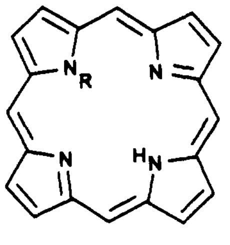

1

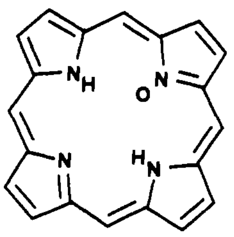

2

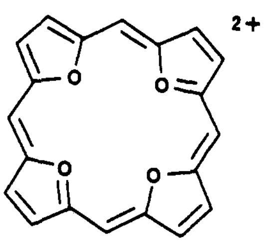

3

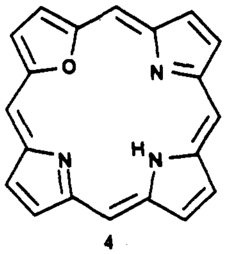

4

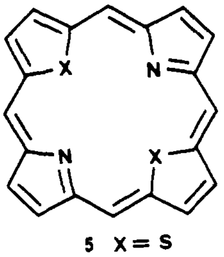

5 X = S
6 X = Se

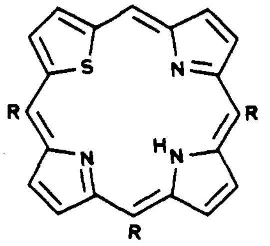

7

[†] University of Wrocław.
[‡] University of California.

0020-1669/89/1328-1183$01.50/0